Pramana – J. Phys. (2018) 91:7
https://doi.org/10.1007/s12043-018-1580-7

The structure of ion-acoustic waves in a low-frequency three-component electron–ion space plasma with two-electron populations

G GOVENDER[1] and S MOOLLA[2,*]

[1]Astrophysics and Cosmology Research Unit, School of Mathematics, Statistics and Computer Science, University of KwaZulu-Natal, Private Bag X54001, Durban 4000, South Africa
[2]School of Chemistry and Physics, University of KwaZulu-Natal, Private Bag X54001, Durban 4000, South Africa
*Corresponding author. E-mail: moollas@ukzn.ac.za

MS received 25 August 2017; revised 21 December 2017; accepted 4 January 2018; published online 6 June 2018

Abstract. Low-frequency ion-acoustic waves are analysed on the ion time-scale, in a three-component electron–ion space plasma. The solitary waves propagate in the positive x direction relative to an ambient magnetic field $\vec{B}_0$ which forms static background for a configuration consisting of cool fluid ions and both warm and hot Boltzmann-distributed electrons with temperatures T_{ic}, T_{ew} and T_{eh}, respectively. We derive linear dispersion relation for the waves by introducing first-order density, pressure and velocity perturbations into the ion fluid equations. Additionally, the variation in the nonlinear structure of the waves are investigated by carrying out a full parametric analysis utilising our numerical code. Our results reveal that ion-acoustic waves exhibit well-defined nonlinear spikes at speeds of $M \geq 2.25$ and an electric field amplitude of $E_0 = 0.85$. It is also shown that low wave speeds ($M \leq 2$), higher densities of the hot electrons, antiparallel drifting of the cool fluid ions, and increased ion temperatures all lead to significant dispersive effects. The ion-acoustic plasma waves featured in this paper have forms that are consistent with those classified as the type-A and type-B broadband electrostatic noise (BEN) observed in the data obtained from earlier satellite missions.

Keywords. Ion-acoustic solitary waves; magnetosphere; ion cyclotron frequency; quasineutrality; space plasmas; wave dispersion.

PACS Nos 94.05.Fg; 94.05.Pt; 94.05.Hk

1. Introduction

Nonlinear wave phenomena in multicomponent plasma configurations has attracted much interest among researchers over the last four decades. In particular, a generous amount of attention has been given to the study of electrostatic solitary waves (ESWs) in systems consisting of electrons and ions and has been shown to have substantial relevance to important problems in mainstream astrophysics. Plasmas having various combinations of electrons and ions are known to occupy many regions of the solar terrestrial environment, planetary magnetospheres, the larger interplanetary medium and the very diffuse interstellar medium of typical galaxies. In the special case of magnetospherical plasma distributions, solitary wave structures are typically observed in the parallel electric field measured relative to the ambient magnetic field, and usually assume bipolar or tripolar forms.

In this paper, we focus our attention on the influence the electron–ion dynamics has on the nonlinearity of low-frequency ESWs that are commonly present within the domain of the Earth's magnetosphere in the plasma sheet boundary layer, the polar cap regions, the magnetosheath and the bow shock generated by the incoming solar wind. Some very important treatments involving these and similar aspects have in recent years been carried out and they include amongst others, the works of [1–6]. It is widely accepted that ESWs can be generated by mechanisms associated with magnetic reconnection and various plasma instabilities such as, bump-on-tail instability, modified two-stream instability, Buneman instability, lower hybrid instability and the beam plasma instability. Various computer

simulations have been utilised to study the general features as well as the generation mechanisms of ESWs in two- and three-component magnetoplasmas. Lu *et al* [7] employed one-dimensional electrostatic particle simulations to study monochromatic electron-acoustic waves in a three-component electron plasma. Their results indicated positive potential signatures and stability for the waves. Kakad *et al* [8] used fluid and particle-in-cell (PIC) simulations to investigate the nonlinear behaviour of ion-acoustic waves in a homogeneous collisionless plasma consisting of fluid electrons and fluid ions, and in an electron–ion plasma (with the electrons and ions governed by the shifted Maxwellian distribution) with periodic boundary conditions, respectively. They demonstrated the importance of full fluid models as well as models that include kinetic effects, in order to have a more complete understanding of the nature of ESWs. Two-dimensional fluid and particle simulations formed the basis of a study by Jao and Hau [9]. They focussed on bi-streaming and bump-on-tail streaming instabilities in electron–ion plasmas. Their results showed that the ambient magnetic field diminished the unstable modes of the bi-streaming instability while the growth rates of the unstable modes of the bump-on-tail instability are enhanced from an increase in the intensity of the ambient magnetic field. In addition to the different simulations that have been used, a wide variety of other types of numerical treatments have also been considered in order to further the modelling of solitary plasma waves. Ghosh *et al* [10] analysed positive amplitude electron-acoustic solitary waves in magnetised plasmas in the context of boundary layers. It was found that ion densities and temperatures importantly determined the essential features and the existence domain of the waves. The Sagdeev pseudopotential technique was used to investigate ion-acoustic structures in a relativistic electron–positron–ion plasma in a study conducted by Tribech and Boukhalfa [11]. They demonstrated that for a fixed flow velocity, the sharpness and the height of the ion-acoustic wave decreases with a corresponding increase in the relativistic electron temperature and on the whole made strong arguments for the existence of ESW structures in astrophysical environments containing plasmas with high bulk flow and particle velocities. Subsequently, Sijo *et al* [12] considered obliquely propagating solitary waves in a five-component cometary plasma. They obtained solutions to the KdV equation and demonstrated that the cold photoelectron component reduced both the wave amplitude and width while the amplitude of the solitary wave increases with increasing solar electron temperatures.

The investigations in our study here in this paper follow on from the earlier work of Lakhina *et al* [13], in which they modelled ion and electron-acoustic solitons in a three-component unmagnetised electron–ion plasma consisting of cold and hot electrons, i.e. two-temperature-defined electron populations, and hot ions. We, on the other hand, consider low-frequency ESWs in a magnetised three-component plasma having cool (not cold) fluid ions and hot and warm Boltzmann-distributed electrons. Our aim is to investigate the influence of the coupled finite-temperature effects and general plasma behaviour on the nonlinear structure of the ion-driven solitary waves. This paper is organised as follows: in §1 we provide the basic theory underlying the plasma model to be studied, in §2 we investigate the linear wave modes of the system by deriving the linear dispersion relation, §3, the most important part of this project, involves the presentation of the details and subsequent results of the nonlinear wave analysis, and finally in §4 we discuss our findings.

2. Formulation of the three-component plasma model

2.1 *Underlying theory*

We consider ESWs in a three-component electron–ion plasma having cool fluid ions with finite non-zero temperature, T_{ic}, and two-electron populations (hot and warm) with temperatures T_{eh} and T_{ew}, respectively, described by the Boltzmann distributions

$$n_{eh} = n_{eh0} \exp\left(\frac{e\phi}{T_{eh}}\right) \tag{1}$$

and

$$n_{ew} = n_{ew0} \exp\left(\frac{e\phi}{T_{ew}}\right), \tag{2}$$

for the hot and warm electrons. In the above equations, n_{eh} is the non-equilibrium density of the hot electrons, n_{eh0} is the equilibrium density of the hot electrons, n_{ew} is the non-equilibrium density of the warm electron species and n_{ew0} is of course the equilibrium density of the warm electrons. The ions are termed as cool and not cold as they have the lowest non-zero temperature amongst the three species, such that $T_{ic} < T_{ew} < T_{eh}$. As usual, e is the electronic charge and ϕ is the unnormalised electrostatic potential of the solitary wave. The ESWs are restricted to propagation in the positive x direction only while the ions are free to drift along the ambient magnetic field lines. Since the ions obey the fluid approximation, the overall plasma dynamics is governed by the time-scale of the heavier slow moving ions, thus requiring a state of quasineutrality over the entire long-term evolution of the system. Consequently,

the ESWs will be defined for low frequencies ($\omega \ll \Omega_e$). This will later on be confirmed in the nonlinear wave analysis. As the ions are cool and $T_{ic} \neq 0$, the full set of ion fluid conservation equations with the inclusion of thermal pressure gradients take the form

$$\frac{\partial n_i}{\partial t} + \frac{\partial (n_i v_{ix})}{\partial x} = 0, \tag{3a}$$

$$\frac{\partial v_{ix}}{\partial t} + v_{ix}\frac{\partial v_{ix}}{\partial x} + \frac{1}{n_i m_i}\frac{\partial p_i}{\partial x} = -\frac{e}{m_i}\frac{\partial \phi}{\partial x} + \Omega_i v_{iy}\sin\theta, \tag{3b}$$

$$\frac{\partial v_{iy}}{\partial t} + v_{ix}\frac{\partial v_{iy}}{\partial x} = \Omega_i v_{iz}\cos\theta - \Omega_i v_{ix}\sin\theta, \tag{3c}$$

$$\frac{\partial v_{iz}}{\partial t} + v_{ix}\frac{\partial v_{iz}}{\partial x} = -\Omega_i v_{iy}\cos\theta, \tag{3d}$$

$$\frac{\partial p_i}{\partial t} + v_{ix}\frac{\partial p_i}{\partial x} + 3p_i\frac{\partial v_{ix}}{\partial x} = 0, \tag{3e}$$

where n_i is the un-normalised ion number density, m_i is the ion mass and Ω_i is the ion cyclotron frequency. The un-normalised ion velocities in the x, y and z directions are given respectively by v_{ix}, v_{iy} and v_{iz}.

In order to successfully complete the nonlinear wave analysis, the fluid equations (3) must be integrated subject to self-consistently determined initial conditions that prevail when the plasma system is in equilibrium. This is achieved by first making a transformation into a stationary frame of the ESW. The dimensionless variable

$$s = \frac{(x - Vt)}{V/\Omega_i} \tag{4}$$

for which V is the un-normalised wave speed and $\Omega_i = eB_0/m_i$, characterises the stationary frame and makes possible the implementation of the RK4 algorithm in our fluid code. The velocities v and V are normalised with respect to the ion-acoustic speed $C_s = \sqrt{T_{eh}/m_i}$. The normalised electric potential ψ of the ESW, is coupled to the electric field E in the following way:

$$\psi = \frac{e\phi}{T_{eh}} \tag{5}$$

$$E = \frac{\partial \psi}{\partial s}. \tag{6}$$

The subscript n will be used to denote quantities that have been normalised. The three-component plasma configuration in our model is asymmetrical and consequently all particle number densities are normalised with respect to the equilibrium ion density n_{i0}. The thermal pressure of the warm fluid ions is normalised with respect to the ambient plasma pressure p_0 that is coupled to the hot electron temperature T_{eh} via the relation $p_0 = n_{i0}T_{eh}$.

2.2 *Evolution equations for the plasma model*

The cool ion fluid equations represented in system (3) are transformed into a stationary frame of the ESW with the aid of the change of variables

$$\frac{\partial}{\partial t} \to -\Omega_e\frac{\partial}{\partial s}$$

and

$$\frac{\partial}{\partial x} \to \left(\frac{\Omega_e}{V}\right)\frac{\partial}{\partial s}.$$

This process eventually leads to five coupled differential equations which collectively describe the overall behaviour of the three-component electron–ion plasma. These governing equations are written as

$$\frac{\partial \psi}{\partial s} = \frac{n_{in}^3 v_{iyn} M\sin\theta}{n_{in}^3 - H\left[\left(\frac{n_{eh0}}{n_{i0}}\right)e^{\psi} + \left(\frac{n_{ew0}}{n_{i0}}\right)\sigma e^{\sigma\psi}\right]}, \tag{7a}$$

$$\frac{\partial n_{in}}{\partial s} = \frac{n_{in}^3[E - v_{iyn}M\sin\theta]}{(M - \delta_i\cos\theta)^2 - 3p_{in}n_{in}}, \tag{7b}$$

$$\frac{\partial p_{in}}{\partial s} = \frac{3p_{in}n_{in}^2[E - v_{iyn}M\sin\theta]}{(M - \delta_i\cos\theta)^2 - 3p_{in}n_{in}}, \tag{7c}$$

$$\frac{\partial v_{iyn}}{\partial s} = \frac{n_{in}M\sin\theta\left[M - \frac{(M-\delta_i\cos\theta)}{n_{in}}\right] - L}{(M - \delta_i\cos\theta)}, \tag{7d}$$

$$\frac{\partial v_{izn}}{\partial s} = \frac{n_{in}v_{iyn}M\cos\theta}{(M - \delta_i\cos\theta)}, \tag{7e}$$

where $H = (M - \delta_i\cos\theta)^2 - 3p_{in}n_{in}$ and the symbol L represents the term $n_{in}v_{izn}M\cos\theta$, for convenience. Note that all quantities appearing above have been written with appropriate normalisations as outlined in the earlier discussion. In the above $M = V/C_s$ is the Mach number of the ESW, n_{eh0}/n_{i0} is the ratio of the equilibrium density of the hot electrons to the ion density and n_{ew0}/n_{i0} is the ratio of the warm electron density to the ion density. The quantity $\delta_i = v_{i0}/C_s$ is the normalised drift velocity of the ion fluid and $\sigma = T_{eh}/T_{ew} > 1$ is the hot to warm electron temperature ratio. In order to study the nonlinear features of the ESWs, one has to generate accurate numerical profiles for the ESW-plasma electric field E. This objective is achieved by numerically integrating the governing system of equations (7) utilising a fourth-order Runge–Kutta (RK4) algorithm [14].

2.3 *Determination of the initial conditions*

The three-component plasma is considered to be locally quasineutral and hence in equilibrium initially at $s = 0$. At this stage, the system is described by the relation $n_{eh0} + n_{ew0} = n_{i0}$ (quasineutrality at $s = 0$) along with

the following additional conditions:

$$\psi = 0, \quad \frac{\partial \psi}{\partial s} = E_0, \quad \frac{\partial^2 \psi}{\partial s^2} = 0, \quad n_i = n_{i0},$$
$$n_{eh} = n_{eh0}, \quad v_{x0} = v_0 \cos\theta, \quad n_{ew} = n_{ew0},$$

for $\psi, n_i, n_{eh}, n_{ew}$ and v_x. E_0 is the uniform driving electric field (at $s = 0$). These crucial plasma parameters are initially assigned values that are within the range of measurements made along the auroral field lines, and for the purpose of our work we adopt in our fluid code the following set of parameter assignments: $n_{ehn0} = 0.5$, $n_{ewn0} = 1 - n_{ehn0} = 0.5$ (due to quasineutrality) and $p_{in0} = T_i/T_{eh} = 0.3$. The normalised ion pressure at $s = 0$ is determined by the cool ion to hot electron temperature ratio, T_i/T_{eh}, and the initial value of 0.3 is in keeping with the fact that the fluid ions are considerably cooler than both the electron species when the system starts to evolve. Consequently, the ion velocities in the y and z directions, v_{iyn} and V_{izn}, respectively, are calculated self-consistently by incorporating the initial values of the preceding parameters mentioned above, in the following equations (valid at the initial point $s = 0$):

$$v_{iyn0} = \frac{E_0}{M\sin\theta}\left\{1 - [\Lambda^2 - 3p_{in}n_{in}]\left(\frac{n_{eh0}}{n_{i0}}\right) - [\Lambda^2 - 3p_{in}n_{in}]\left(\frac{n_{ew0}}{n_{i0}}\right)\frac{T_{eh}}{T_{ew}}\right\}, \tag{8}$$

$$\Gamma = \frac{3E_0\frac{\partial n_{in}}{\partial s}}{\Lambda^2 - 3p_{in}n_{in}} + \frac{3E_0\left[\frac{\partial p_{in}}{\partial s} + p_{in}\frac{\partial n_{in}}{\partial s}\right]}{[\Lambda^2 - 3p_{in}n_{in}]^2} - \frac{3v_{iyn}M\sin\theta\frac{\partial n_{in}}{\partial s}}{\Lambda^2 - 3p_{in}n_{in}} - \frac{3v_{iyn}M\sin\theta\left[\frac{\partial p_{in}}{\partial s} + p_{in}\frac{\partial n_{in}}{\partial s}\right]}{[\Lambda^2 - 3p_{in}n_{in}]^2}, \tag{9}$$

$$\frac{\partial v_{iyn0}}{\partial s} = \frac{1}{M\sin\theta}[\Lambda^2 - 3p_{in}n_{in}]\left[\Gamma - E_0^2 \times \left(\frac{n_{eh0}}{n_{i0}}\right) - E_0^2\left(\frac{n_{ew0}}{n_{i0}}\right)\left(\frac{T_{eh}}{T_{ew}}\right)^2\right], \tag{10}$$

$$v_{izn0} = \frac{\sin\theta}{\cos\theta}(M - \Lambda) - \frac{\Lambda}{M\cos\theta}\frac{\partial v_{iyn0}}{\partial s}, \tag{11}$$

where $\Lambda = M - \delta_i\cos\theta$ and Γ have been defined for simplicity. These equations, together with the normalised ion fluid system (7), completely describe the coupling between the ESW and the dynamics of the three-species plasma. They will be analysed later on with our fluid code, and their solutions will be valuable in our investigations of the electron and ion influence on the nonlinear wave structures.

3. Derivation of the linearised dispersion relation $\omega(k)$

The linear wave modes of the system are now explored by generating the dispersion relation $\omega(k)$. We follow the method presented by Chen [15]. First, perturbations to first order in the density, velocity, pressure and wave potential, of the form $n_i = n_{i0} + n_{i1}, v_{ij} = v_{ij0} + v_{ij1}(j = x, y, z), p_i = p_{i0} + p_{i1}, \phi = \phi_0 + \phi_1$ are introduced into the fluid equations. This process is closed by choosing the basic wave form $\exp[i(kx - \omega t)]$ which generates the derivatives $(\partial/\partial t) = -i\omega$ and $(\partial/\partial x) = ik$. The linearisation is considered at the initial point $s = 0$ where the bulk plasma configuration and the individual constituents are stationary so that the following restrictions, $\nabla n_{i0} = 0, \nabla p_{i0} = 0$, and $(\partial/\partial t)p_{i0} = 0 = (\partial/\partial t)n_{i0}$, hold. These assumptions, together with the linearisation and the quasineutrality condition, lead to the intermediate result

$$n_{eh0}\left(\frac{e\phi}{T_{eh}}\right) + n_{ew0}\left(\frac{e\phi}{T_{ew}}\right) = \frac{k^2 n_{i0} e\phi}{\omega^2 m_i - 3k^2 T_i - \frac{\omega m_i \Omega_i^2 \sin^2\theta}{\omega - (\Omega_i^2/\omega)\cos^2\theta}},$$

where the hot and warm Boltzmann-distributed electron densities (1) and (2), respectively, have been expanded to first order in $e\phi/T_{eh}$ and $e\phi/T_{ew}$. After appropriate algebraic manipulations, the above equation finally yields the linear wave dispersion relation of the form

$$\omega_\pm^2(k) = \frac{1}{2}[\Omega_i^2 + 3k^2 v_{ti}^2 + \alpha] \pm \frac{1}{2}[(\Omega_i^2 + 3k^2 v_{ti}^2 + \alpha)^2 - 4(3k^2 v_{ti}^2 + \alpha)\Omega_i^2\cos^2\theta]^{1/2}, \tag{12}$$

where

$$\alpha = \frac{k^2 C_s^2\,(n_{i0}/T_{eh})}{(n_{eh0}/T_{eh}) + (n_{ew0}/T_{ew})}$$

has been defined for convenience and $v_{ti} = (T_i/m_i)^{1/2}$ is the ion thermal speed. The relatively higher ion cyclotron frequency is represented by $\omega_+^2(k)$ while the lower ion-acoustic frequency is described by $\omega_-^2(k)$. Both these subfrequency scales are contained within the larger low-frequency scale that is defined by the more massive slow moving ions. It will be made very clear in the nonlinear wave analysis to follow, that the three-component electron–ion plasma we are studying admits ESWs lying only in the relatively lower frequency ion-acoustic subscale.

4. Nonlinear wave analysis

4.1 *The linear, sawtooth and nonlinear 'spiky' wave structures*

At the beginning of the nonlinear wave analysis, it is important to identify the three basic wave forms that are typical in such a plasma system. In order to achieve this task, the driving electric field E_0 is increased steadily while the remaining plasma parameters are kept fixed. This process should in principle identify three critical values at which the ESWs assume linear, bipolar or 'sawtooth' and 'highly nonlinear spiky' features. We are most interested in the influence of plasma dynamics on the nonlinear spikes because it is precisely these structures that appear quiet prominently in the data collected from various satellite missions. What is also noteworthy is that in many such variations of E_0, one or more transitions between the low- and high-frequency modes may be observed. However, this is not always the case. The numerical profiles displayed in figure 1 shows the linear sine wave form at $E_0 = 0.01$ (a), the 'sawtooth' structure occurring at $E_0 = 0.5$ (b) and most importantly the very pronounced nonlinear spikes emerging at an amplitude of $E_0 = 0.85$ (c). These wave profiles are generated for a fixed parameter background such that $M = 2.25$, $\theta = 2°$, $\delta_i = 0.0$ (no drifting motion of the ions), $n_{eh0}/n_{i0} = 0.5$, $n_{ew0}/n_{i0} = 0.5$, $T_i/T_{eh} = 0.3$ and $T_{eh}/T_{ew} = 1.5$. A driving electric field of $E_0 = 0.01$ yields a linear ion-acoustic wave with period $\tau_{\mathrm{ESW}} \approx 1.02\tau_{ci}$, while $E_0 = 0.5$ and $E_0 = 0.85$ produce 'sawtooth' and 'spiky nonlinear' ion-acoustic waves having periods $2.109\tau_{ci}$ and $3.805\tau_{ci}$, respectively, where $\tau_{ci} = 2\pi/\Omega_i$ is the ion cyclotron frequency. In the transition for the linear sine wave to the nonlinear spiky form, the change in wave period is $\Delta\tau_{\mathrm{ESW}} \approx 2.065\tau_{ci}$ which is too large to allow for the waves for transition into the ion cyclotron subscale. In fact, as we shall soon see, the waves in this particular model will have periods in excess of the ion cyclotron period τ_{ci} and thus will always be defined in the lower ion-acoustic subfrequency scale.

4.2 *The influence of the wave speed M on the nonlinear structures*

Next in our nonlinear analysis, we explore any effect the Mach number M may have on the nonlinearity of the solitary wave structures. By keeping the driving electric field E_0 fixed at 0.85 for well-defined nonlinear waveforms, we vary the wave speed over the intervals [2.25,15] for supersonic ESWs and [2.25,1.75] for subsonic waves. We find from the numerical outputs generated in figure 2 that when M is increased from 5 to 15, the ion-acoustic waves have a resulting change in period of the order of $\Delta\tau_{\mathrm{ESW}} \approx 0.08\tau_{ci}$. This substantial increase in the Mach number has only a small effect on the wave periods and results in a very slight compression of the ESWs. On the other hand, reducing the wave speed from $M = 2$ to $M = 1.75$ has a more dramatic influence on the nonlinear structures as seen in figures 3a and 3b. In this regard, the period increases from $3.923\tau_{ci}$ to $4.15\tau_{ci}$ inducing a significant broadening of the profiles. It is interesting to note that for this particular model, any further decrease in M causes the solitary waveforms to depart from their nonlinear shapes.

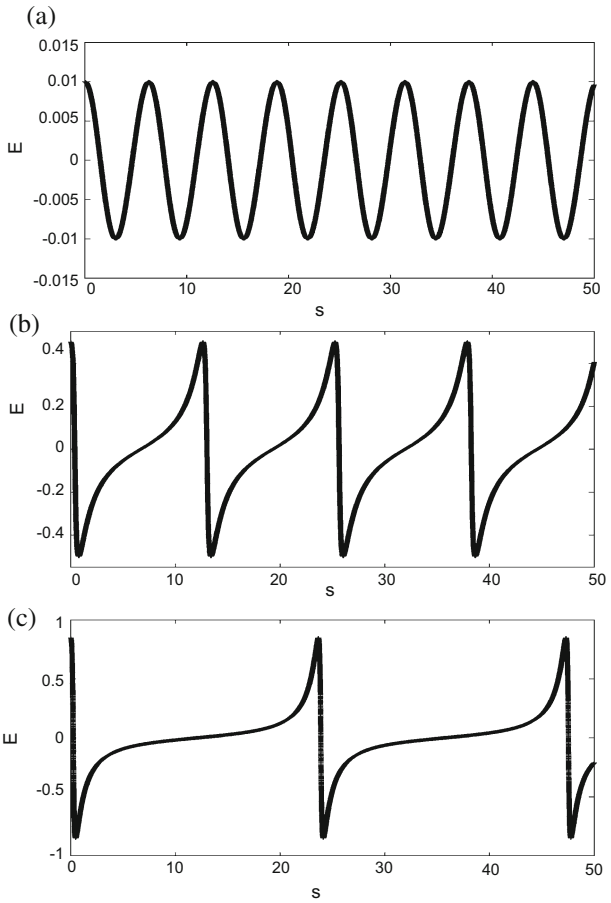

Figure 1. The variation of the electric field amplitude, when $M = 2.25$, $\theta = 2°$, $\delta_i = 0.0$, $n_{eh0}/n_{i0} = 0.5$, $n_{ew0}/n_{i0} = 0.5$, $T_i/T_{eh} = 0.3$, $T_{eh}/T_{ew} = 1.5$. (**a**) $E_0 = 0.01$ linear, (**b**) $E_0 = 0.5$ 'sawtooth', (**c**) $E_0 = 0.85$ 'spiky nonlinear'.

4.3 *The influence of the hot electrons at equilibrium, on the nonlinear solitary structures*

To investigate the effects of hot and warm electrons at $s = 0$ on the ion-acoustic waves, one has to consider the parametric variation of the hot electron density

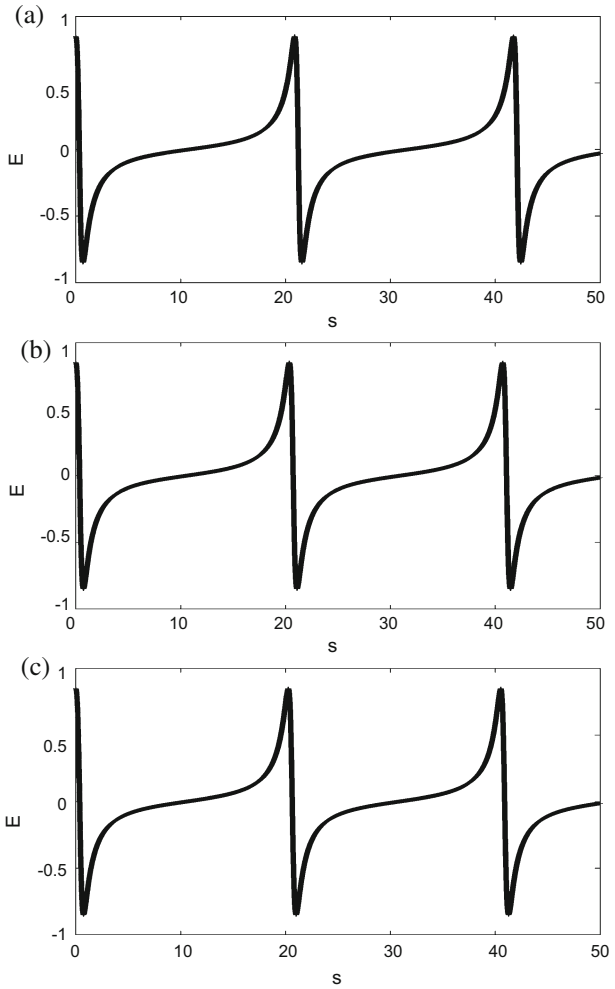

Figure 2. Fluctuations in the nonlinear wave structures for increasing wave speeds when $E_0 = 0.85$, $\delta_i = 0.0$, $n_{eh0}/n_{i0} = 0.5$, $n_{ew0}/n_{i0} = 0.5$, $T_i/T_{eh} = 0.3$, $T_{eh}/T_{ew} = 1.5$ and $\theta = 2°$. (**a**) $M = 5$, (**b**) $M = 10$, (**c**) $M = 15$.

$n_{ehn0} = n_{eh0}/n_{i0}$ and the warm electron density $n_{ewn0} = n_{ew0}/n_{i0}$. However, as these are coupled to each other via equation $n_{ehn0} + n_{ewn0} = 1$, arising, again, from quasineutrality at $s = 0$, it is sufficient only to consider fluctuations in just one of these. We investigate the nature of nonlinearity of the waves by focussing on the steady decrease in the hot electron species due to the fact that they will lose energy over time. Figure 4 displays the wave structures generated by decreasing n_{ehn0} over the interval [0.5, 0.1]. The structure in figure 4a corresponds to the ion-acoustic wave when $n_{ehn0} = n_{ewn0} = 0.5$, due to quasineutrality. The wave period here is measured to be $3.805\tau_{ci}$, while from figure 4b it is found that $n_{ehn0} = 0.3$ produces a wave having a larger period of $\tau_{\mathrm{ESW}} \approx 4.20\tau_{ci}$. The period measured from the profile in figure 4c is of the order of

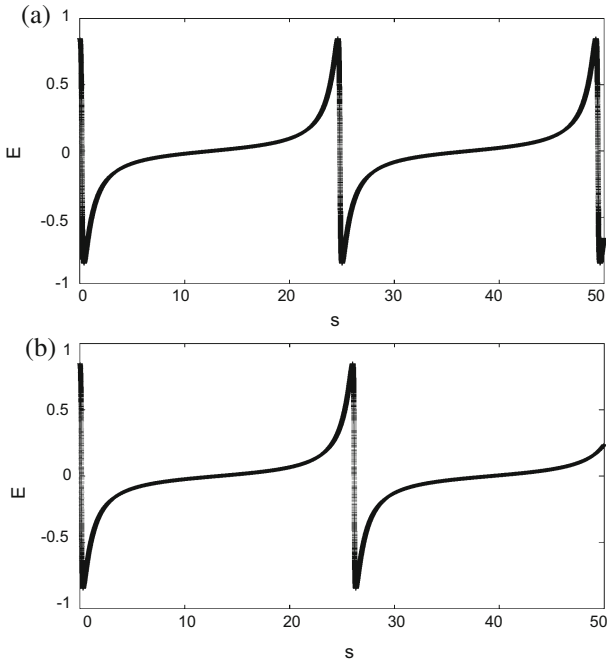

Figure 3. Fluctuations in the nonlinear wave structures for decreasing wave speeds when $E_0 = 0.85$, $\delta_i = 0.0$, $n_{eh0}/n_{i0} = 0.5$, $n_{ew0}/n_{i0} = 0.5$, $T_i/T_{eh} = 0.3$, $T_{eh}/T_{ew} = 1.5$ and $\theta = 2°$. (**a**) $M = 2$ and (**b**) $M = 1.75$.

$4.70\tau_{ci}$ which arises from a markedly lower hot electron density given by $n_{ehn0} = 0.1$. It can be seen clearly from these measurements that as the density of initially hot electrons reduce due to cooling, the wave periods become increasingly larger and give rise to the scaling law $\tau_{\mathrm{ESW}} \propto 1/n_{ehn0}$.

4.4 *The impact of increasing propagation angle*

The three-component electron–ion plasma model in this study has been defined for almost parallel propagating $\theta = 2°$ monochromatic ion-acoustic solitary waves. However, as the plasma starts to evolve and departs from its equilibrium state at $s = 0$ the angle θ may change. Hence, it is worthwhile exploring any influence the angle of propagation may have on the nonlinearity of the ESW structures. The wave profiles illustrated in figures 5a–5d are due to $\theta = 2°$, $\theta = 20°$, $\theta = 40°$ and $\theta = 60°$, respectively. Over the interval [2, 60] degrees, the period changes only by a small amount $\Delta\tau_{\mathrm{ESW}} \approx 0.08\tau_{ci}$ which results in a very slight compression of the wave. For the particular plasma set-up in our investigations, we observe, in general, that while variations in the propagation angle do not have a substantial influence on the nonlinear characteristics of the ESWs, the model itself still allows for larger angles and thus non-parallel motion of the waves.

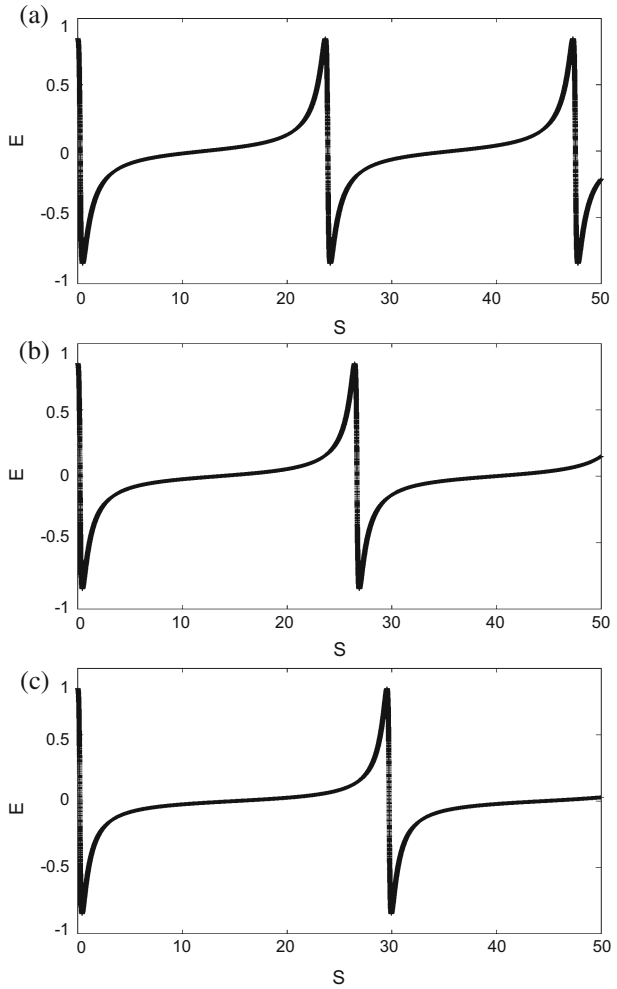

Figure 4. Fluctuations in the nonlinear wave structures for decreasing hot electron density when $E_0 = 0.85$, $\delta_i = 0.0$, $T_i/T_{eh} = 0.3$, $T_{eh}/T_{ew} = 1.5$, $M = 2.25$ and $\theta = 2°$. (**a**) $n_{eh0}/n_{i0} = 0.5$, (**b**) $n_{eh0}/n_{i0} = 0.3$, (**c**) $n_{eh0}/n_{i0} = 0.1$.

4.5 *Analysing the drifting motion of the cool fluid ions*

It has been previously shown that the drifting motion of fluid particles along the ambient magnetic field lines can often play a huge role in contributing towards wave dispersion and variations in the nonlinearity of electrostatic plasma waves. To study the full impact of drifting, one has to consider both parallel drift velocities ($\delta > 0$) which correspond to fluid flow in the wave direction, and antiparallel drift velocities ($\delta < 0$) which describe fluid flow against the direction of wave motion. In a model by Reddy *et al* [16] where they considered coupled nonlinear ion cyclotron and ion-acoustic waves in a two-component electron ion plasma, it was demonstrated that antiparallel ion drifts resulted in significant broadening of the waves while parallel ion drifts produced appreciable wave compression. Similar trends were reported by Moolla *et al* [17] in a

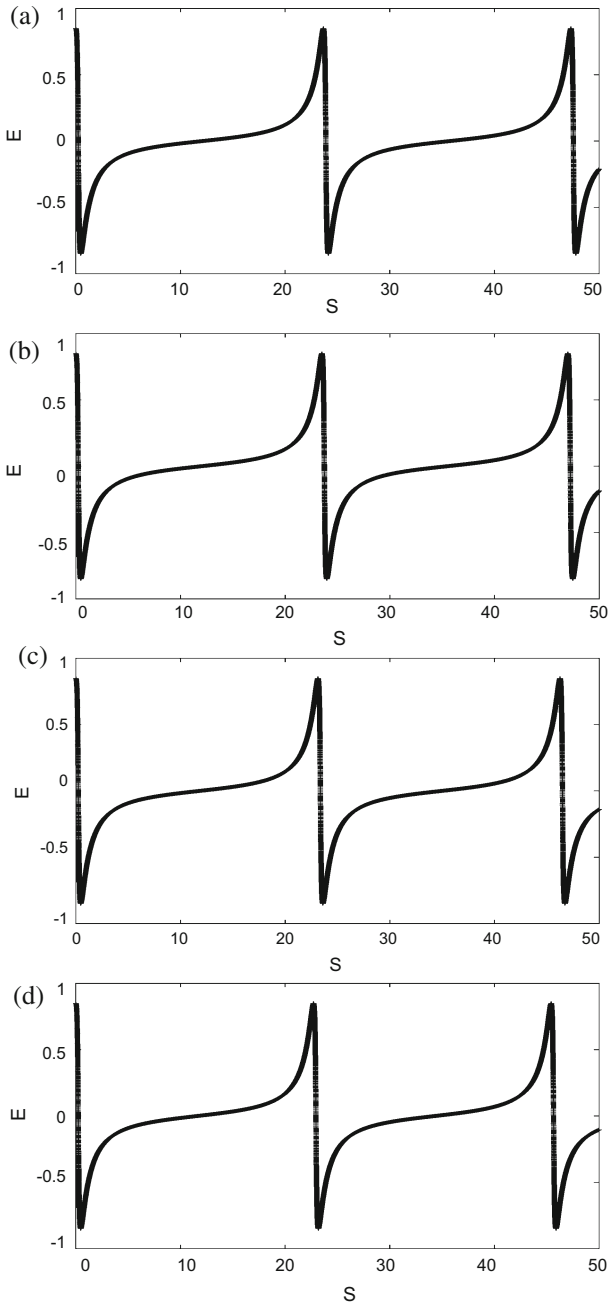

Figure 5. Fluctuations in the nonlinear wave structures for increasing propagation angle when $E_0 = 0.85$, $\delta_i = 0.0$, $n_{eh0}/n_{i0} = 0.5$, $n_{ew0}/n_{i0} = 0.5$, $T_i/T_{eh} = 0.3$, $T_{eh}/T_{ew} = 1.5$ and $M = 2.25$. (**a**) $\theta = 2°$, (**b**) $\theta = 20°$, (**c**) $\theta = 40°$, (**d**) $\theta = 60°$.

study of high-frequency waves in a three-component magnetoplasma consisting of hot electrons, cold electrons and cold ions modelled in the fluid approximation with the inclusion of charge separation effects. Figure 6 depicts the wave profiles associated with parallel ion drifts such that $\delta_i = 0.4$ (a) and $\delta_i = 0.8$ (b). It can be clearly observed that an increase in the ion drift

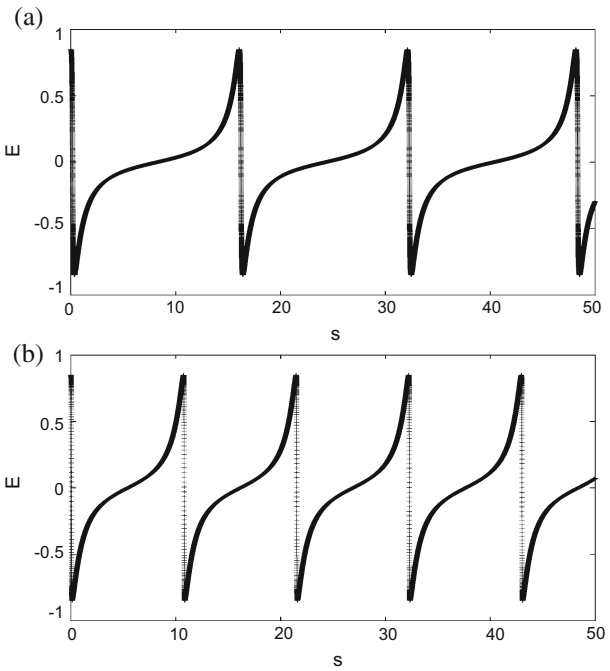

Figure 6. Fluctuations in the nonlinear wave structures corresponding to the parallel drifting motion of the fluid ions when $E_0 = 0.85$, $n_{eh0}/n_{i0} = 0.5$, $n_{ew0}/n_{i0} = 0.5$, $T_i/T_{eh} = 0.3$, $T_{eh}/T_{ew} = 1.5$, $M = 2.25$ and $\theta = 2°$. (**a**) $\delta_i = 0.4$ and (**b**) $\delta_i = 0.8$.

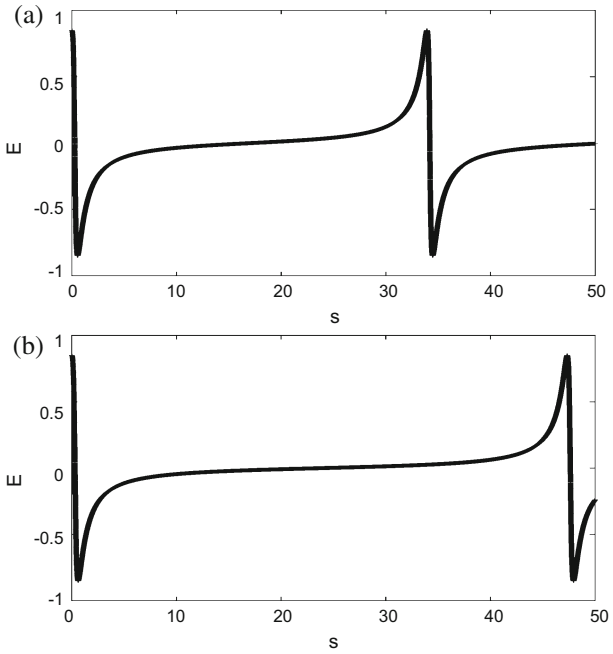

Figure 7. Fluctuations in the nonlinear wave structures corresponding to the antiparallel drifting motion of the fluid ions when $E_0 = 0.85$, $n_{eh0}/n_{i0} = 0.5$, $n_{ew0}/n_{i0} = 0.5$, $T_i/T_{eh} = 0.3$, $T_{eh}/T_{ew} = 1.5$, $M = 2.25$ and $\theta = 2°$. (**a**) $\delta_i = -0.4$ and (**b**) $\delta_i = -0.8$.

velocity δ_i leads to a generous increase in the wave frequency ω, with a change in period of $\Delta\tau_{\mathrm{ESW}} \approx 0.86\tau_{ci}$. The waveforms in figure 7, on the other hand, correspond to antiparallel ion drifts with $\delta_i = -0.4$ and $\delta_i = -0.8$ represented in (a) and (b), respectively. It is very clear that the antiparallel fluid ion flow in our model generates ESWs that exhibit the very same dispersive features that are consistent with those found in the models investigated by Reddy *et al* [16] and Moolla *et al* [17]. Moreover, it is remarkable from the electric field structures in figure 7, that for $\delta_i < 0$ the wave periods fluctuate dramatically with the change in period given by $\Delta\tau_{\mathrm{ESW}} \approx 2.14\tau_{ci}$. It appears that for our model, antiparallel ion drifts lead to very pronounced dispersive effects.

4.6 *Finite non-zero temperature effects of the ion fluid*

As the cool fluid ions are at the lowest temperature in the three-component configuration ($T_{eh} > T_{ew} > T_{ic}$), the ions, over a period of time, should experience an increase in temperature and eventually reach a state of thermal equilibrium with the remaining two particle components. Thus, it is worthwhile to actually investigate any effect that the increasing ion temperature may have on the form of the nonlinear ESW structures. Finite non-zero temperatures are known to be responsible for inducing dispersion in plasma waves. We follow the growth of the ion temperature by tracking the fluctuations in the ion temperature to hot electron temperature ratio T_i/T_{eh} from its equilibrium value 0.3 at $s = 0$ up to the value of $T_i/T_{eh} = 0.6$ at which point the ions have gained sufficient energy from the electrons. Figure 8 shows the numerical waveforms depicting variations in the nonlinearity of the ion-acoustic structures as T_i increases steadily. The graphic in figure 8a displays the 'spiky' nonlinear structure generated when $E_0 = 0.85$ and $T_i/T_{eh} = 0.3$. This wave has a period of $3.805\tau_{ci}$. The graphic in figure 8b depicts the nonlinear wave when $T_i/T_{eh} = 0.6$. As the ratio of the ion temperature to the temperature of the hot electrons increases from 0.3 to 0.6, the ESW has a change in period of the order of $0.87\tau_{ci}$. This is sufficient to bring about the onset of the dispersive features observed in figure 8b. It can be deduced easily that the coupling between the ion temperature and the wave period can be described by the relation $\tau_{\mathrm{ESW}} \propto T_i$.

4.7 *The impact of hot electrons on the nonlinearity of the ion-acoustic ESWs*

At $s = 0$, when the plasma is in equilibrium, the hot electron species with temperature T_{eh} is coupled

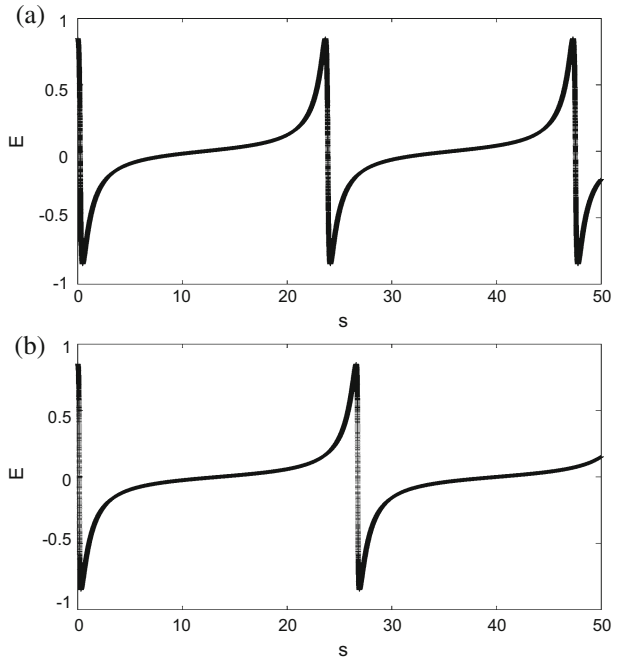

Figure 8. Fluctuations in the nonlinear wave structures corresponding to increasing ion fluid temperature when $E_0 = 0.85$, $\delta_i = 0.0$, $n_{eh0}/n_{i0} = 0.5$, $n_{ew0}/n_{i0} = 0.5$, $T_{eh}/T_{ew} = 1.5$, $M = 2.25$ and $\theta = 2°$. (**a**) $T_i/T_{eh} = 0.3$ and (**b**) $T_i/T_{eh} = 0.6$.

to the warm electrons with temperature T_{ew} as defined in the ratio $T_{eh}/T_{ew} = \sigma > 1$. This factor appears in the conservation equations for the ion fluid (7) and eqs (8) through (11) which are used to determine self-consistently, the initial conditions of the system. It is however possible that as the plasma starts to evolve and departs from its initial state at $s = 0$, the hotter electrons may cool down until such time that they are in thermal equilibrium with the original distribution of warm electrons ($T_{eh} \rightarrow T_{ew}$) and this process may in turn give rise to notable fluctuations in the degree of nonlinearity of the ion-acoustic wave structures. This can be better understood by analysing the decrease in the ratio T_{eh}/T_{ew}. The numerical solutions presented in figure 9 give variations in the normalised electric field of the ion-acoustic waves when the hot to warm electron temperature ratio is reduced from its initial value of 1.5 to 1.0 when the two-electron components are at the same temperature. Correspondingly, the periods of the waves decrease from $3.805\tau_{ci}$ to $2.86\tau_{ci}$. The results in figure 9 clearly indicate the resulting compression and increase in frequency ω of the waves as the hot electrons cool down and the wave period τ_{ESW} decreases proportionally. This behaviour can be described using the relation $\tau_{\mathrm{ESW}} \propto T_{eh}$.

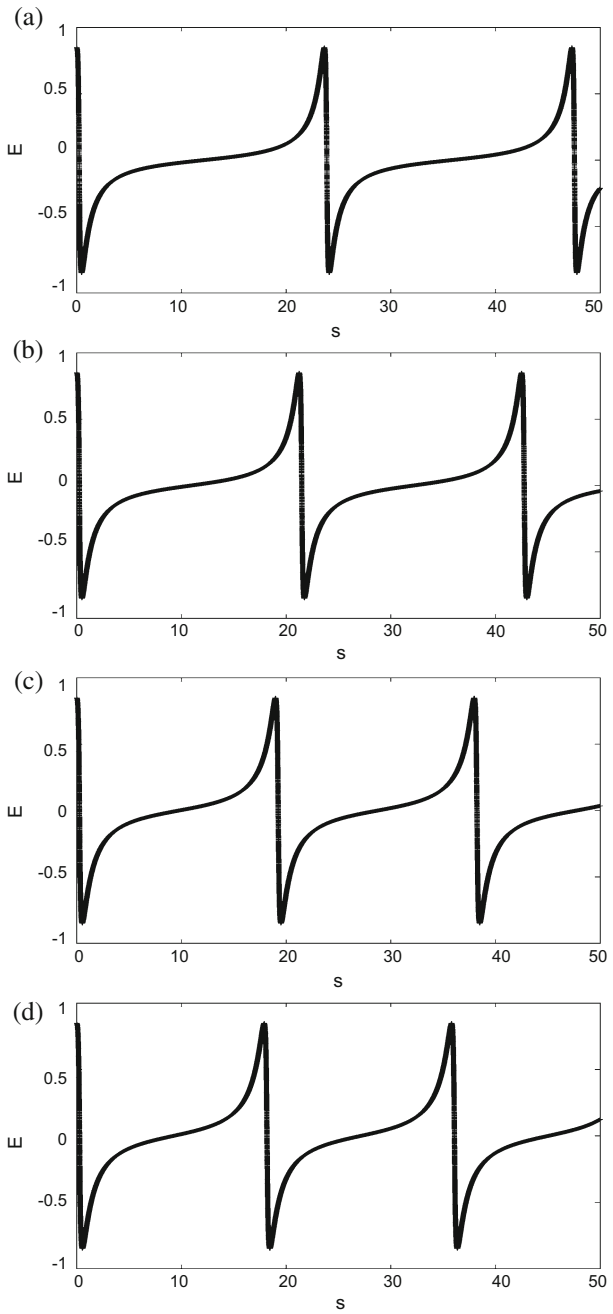

Figure 9. Fluctuations in the nonlinear wave structures for a decrease in the hot electron temperature when $E_0 = 0.85$, $\delta_i = 0.0$, $n_{eh0}/n_{i0} = 0.5$, $n_{ew0}/n_{i0} = 0.5$, $T_i/T_{eh} = 0.3$, $M = 2.25$ and $\theta = 2°$. (**a**) $T_{eh}/T_{ew} = 1.5$, (**b**) $T_{eh}/T_{ew} = 1.3$, (**c**) $T_{eh}/T_{ew} = 1.1$, (**d**) $T_{eh}/T_{ew} = 1.0$.

5. Conclusion

This research article has been largely concerned with the nonlinear fluctuations of ESWs in a three-component plasma. We have considered a configuration consisting of two-temperature defined electron populations (hot

and warm Boltzmann-distributed electrons) and a cool ion fluid component. In our model, the ion thermal pressure has been taken into account and the condition of quasineutrality has been imposed throughout the evolution of the ESW-plasma system as we are working on the low-frequency time-scale defined by the slow moving ions such that the solitary wave frequency ω is not comparable to the electron cyclotron frequency ($\omega \ll \Omega_e$). In order to investigate the influence of plasma dynamics on the nonlinearity of the waves, we have transformed the ion fluid conservation equations to a stationary frame of the ESW, normalised all densities, velocities and pressures appropriately and finally utilised a fourth-order Runge–Kutta algorithm, subject to self-consistent initial conditions at equilibrium ($s = 0$) to find solutions to the fluid equations.

The numerical solutions admit three critical values for the driving electric field E_0, at which the normalised parallel component of the ESW electric field E exhibits linear sine, 'sawtooth' and 'spiky' nonlinear structures. As the waves are driven from the initial plasma state, an increase in E_0 reveals that linear waveforms occur at $E_0 = 0.01$, 'sawtooth' features appear at $E_0 = 0.5$ and well-defined nonlinear 'spiky' structures dominate at $E_0 = 0.85$. These basic waveforms turn out to have frequencies in the ion-acoustic subscale. Furthermore, we have found from our subsequent parametric analysis, that transitions between the relatively higher frequency ion cyclotron mode and relatively lower frequency ion acoustic mode are not possible for our model and consequently, all nonlinear structures considered have been in the form of ion-acoustic ESWs. We have carried out a detailed nonlinear analysis which has revealed interesting and useful information concerning ion-acoustic solitary waves in a three-component electron–ion plasma. It has been observed that the model allows for both subsonic and supersonic ion-acoustic waves. Higher wave speeds $M \geq 5$ result in slowly decreasing wave periods while low speeds $M \leq 2.25$ yield structures with dramatically increasing periods and thus more enhanced broadening of the profiles. The hot electron population has also been found to have a notable influence on the degree of nonlinearity. A steady reduction in the normalised equilibrium density of the hot electrons contributes significantly to larger periods and thus allows for the ion-acoustic mode to be more pronounced. On the other hand, as the initially hotter electron distribution cools down, the waves become increasingly more compressed and a gradual transition from the very sharp nonlinear 'spikes' to the more intermediate bipolar waveform occurs. We have also found that larger wave propagation angles are possible in the configuration and that for non-parallel wave motion ($2 \ll \theta < 90$) degrees the ion-acoustic waves experience only small decreases in period. The cool ion fluid has also shown to have significant impact on the overall form of the ESWs. First, the parallel and antiparallel drifting motion of the ions have produced similar trends that have been observed previously in the low-frequency results of Reddy *et al* [16] for a two-component electron–ion plasma, and Moolla *et al* [17] who explored high-frequency fluctuations on the electron time-scale, in a three-species electron–ion fluid model. We have demonstrated that for $\delta_i > 0$, the wave profiles are increasingly compressed and hence have sharper increase in frequency, while $\delta_i < 0$ leads to very enhanced broadening such that $\omega \ll \Omega_i$. The effects of an increasing ion temperature were also considered, and our analysis has clearly indicated that as the ions become warmer (due to the presence of two hotter electron components), the ion-acoustic structures have substantial increases in period thus enabling them to exhibit well-defined dispersive features. It is noteworthy that a decreasing hot electron population, the antiparallel ion drifting, and increasing ion temperatures all collectively contribute towards dispersion of the ion-acoustic waves.

Our findings, on the low-frequency ion time-scale, bear resemblance to some features for high-frequency ESWs that characterise the type-A, type-B and type-C BEN that has been well-detected in the satellite data obtained from the VIKING [18], GEOTAIL [19,20], POLAR [21], FAST [22] and CLUSTER [23] space missions. Consequently, the model we have explored would be relevant for possible plasma configurations and their associated nonlinear wave phenomena, that arise naturally in various regions of the Earth's magnetosphere. In conclusion, we point out that most recently, Mugemana *et al* [24] studied low-frequency waves in a three-component electron–ion–positron plasma including the effects of charge separation. Their results also showed a transition from linear to sawtooth to spiky waveforms as the driving electric field increased. They demonstrated that the onset of spiky waveforms occurred at a driving electric field value of $E_0 = 0.3$ whereas in our case nonlinear structures were obtained at a much higher value of $E_0 = 0.85$. This could be due to the coupled effects of charge separation as well as the significant difference in positron and ion masses. On the other hand, in the findings of Reddy *et al* [16] the onset of spiky forms occurred at $E_0 = 1.1$ which is higher than what we have obtained. Additionally, in the investigations of Reddy *et al* [25] which involved electrons, protons and oxygen ion beams, ion-acoustic waves were formed at amplitudes of $E_0 = 0.8$ which is in good agreement with the values in our studies. This also again implies that quasineutrality may possibly allow solitary structures to be driven from much higher initial values.

Acknowledgements

G Govender and S Moolla would like to thank the University of KwaZulu-Natal for the financial and administrative support. They also wish to acknowledge Dr R B Narain from the Astrophysics and Cosmology Research Unit (ACRU) in the School of Mathematics, Statistics and Computer Science, for useful and insightful discussions during the period of this research project.

References

[1] J R Franz, P M Kintner and J S Pickett, *Geophys. Res. Lett.* **25**, 1277 (1998)
[2] B T Tsurutani, C M Ho, G S Lakhina, B Buti, J K Arballo, J S Pickett and D A Gurnett, *Geophys. Res. Lett.* **25**, 4117 (1998)
[3] J S Pickett, L J Chen, R L Mutel, I W Christopher, O Santolik, G S Lakhina, S V Singh, R V Reddy, D A Gurnett, B T Tsurutani, E Lucek and B Lavraud, *Adv. Space Res.* **41**, 1666 (2008)
[4] S V Singh, G S Lakhina, R Bharuthram and S R Pillay, *Phys. Plasmas* **18**, 122306 (2011)
[5] L Shi-You, Z Shi-Feng, D Xiao-Hua and C Hong, *Chin. Phys. Lett.* **29**, 089402 (2012)
[6] A Kakad, B Kakad, C Anekallu, G S Lakhina, Y Omura and A Fazakerely, *J. Geophys. Res. Space Phys.* **121**, 4452 (2016)
[7] Q M Lu, D Y Wang and S Wang, *J. Geophys. Res.* **110**, A03223 (2005)
[8] B Kakad, A Kakad and Y Omura, *J. Geophys. Res. Space Phys.* **119**, 5589 (2014)
[9] C S Jao and L N Hau, *Phys. Plasmas* **23**, 112110 (2016)
[10] S S Ghosh, J S Pickett, G S Lakhina, J D Winningham, B Lavraud and P M E Decreau, *J. Geophys. Res.* **113**, A06218 (2008)
[11] M Tribeche and S Boukhalfa, *Astrophys. Space Sci.* **332**, 279 (2011)
[12] S Sijo, M Manesh, G Sreekala, T W Neethu, G Renuka and C Venugopal, *Phys. Plasmas* **22**, 123704 (2015)
[13] G S Lakhina, A P Kakad, S V Singh and F Verheest, *Phys. Plasmas* **15**, 062903 (2008)
[14] W H Press, S A Teukolsky, W T Vetterling and B P Flannery, *Numerical recipes in Fortran 90 – The art of parallel scientific computing* (Cambridge University Press, New York, 1996) Vol. 2, pp. 702–704, p. 1308
[15] F F Chen, *Introduction to plasma physics and controlled fusion* (Springer, New York, 1983) Vol. 1, pp. 84, 85
[16] R V Reddy, G S Lakhina, N Singh and R Bharuthram, *Nonl. Proc. Geophys.* **9**, 25 (2002)
[17] S Moolla, R Bharuthram, S V Singh and G S Lakhina, *Pramana – J. Phys.* **61**, 1209 (2003)
[18] R G Bostrom, B Gustafsson, G Holback, H Holmgren and P Koskinen, *Phys. Rev. Lett.* **61**, 82 (1998)
[19] H Matsumoto, H Kojima, T Miyatake, Y Omura, M Okada, I Nagano and M Tsutsui, *Geophys. Res. Lett.* **21**, 2915 (1994)
[20] H Matsumoto, I Nagano, R R Anderson, H Kojima, K Hashimoto, M Tsutsui, T Okada, I Kimura, Y Omura and M Okada, *J. Geomag. Geoelectr.* **46**, 59 (1994)
[21] F S Mozer, R Ergun, M Temerin, C Catell, J Dombeck and J Wygant, *Phys. Rev. Lett.* **79**, 1281 (1997)
[22] R E Ergun, C W Carlson, J P McFadden, F S Mozer, G T Delory, W Peria, C C Chaston, M Temerin, I Roth, L Muschietti, R Elphic, R Strangeway, R Pfaff, C A Cattell, D Klumpar, E Shelley, W Peterson, E Moebius and L Kistler, *Geophys. Res. Lett.* **25**, 2041 (1998)
[23] J S Pickett, S W Kahler, L J Chen, R L Huff, O Santolik, Y Khotyaaintsev, P M E Decreau, D Winningham, R Frahm, M L Goldstein, G S Lakhina, B T Tsurutani, B Lavraud, D A Gurnett, M Andre, A Fazakerely, A Balogh and H Reme, *Nonlin. Proc. Geophys.* **11**, 183 (2004)
[24] A Mugemana, S Moolla and I J Lazarus, *Pramana – J. Phys.* **88**, 23 (2017)
[25] R V Reddy, S V Singh, G S Lakhina and R Bharuthram, *Earth Planet Space* **58**, 1227 (2006)